

# Right Place, Right Time!

## Generalizing ObjectNav to Dynamic Environments with Portable Targets

Vishnu Sashank Dorbala\*

Bhrij Patel\*

Amrit Singh Bedi

Dinesh Manocha

University of Maryland, College Park

### Abstract

*ObjectNav is a popular task in Embodied AI, where an agent navigates to a target object in an unseen environment. Prior literature makes the assumption of a static environment with stationary objects, which lacks realism. To address this, we present a novel formulation to generalize ObjectNav to dynamic environments with non-stationary objects, and refer to it as Portable ObjectNav or P-ObjectNav. In our formulation, we first address several challenging issues with dynamizing existing topological scene graphs by developing a novel method that introduces multiple transition behaviors to portable objects in the scene. We use this technique to dynamize Matterport3D, a popular simulator for evaluating embodied tasks. We then present a benchmark for P-ObjectNav using a combination of heuristic, reinforcement learning, and Large Language Model (LLM)-based navigation approaches on the dynamized environment, while introducing novel evaluation metrics tailored for our task. Our work fundamentally challenges the “static-environment” notion of prior ObjectNav work; the code and dataset for P-ObjectNav will be made publicly available to foster research on embodied navigation in dynamic scenes. We provide an anonymized repository for our code and dataset: <https://anonymous.4open.science/r/PObjectNav-1C6D>.*

### 1. Introduction

ObjectNav is a popular embodied navigation task involving an agent finding a label-specified target object in an unseen environment [4, 44, 62]. In this task, an agent is tasked with navigating to an instance of a specified target object class, such as “couch” or “fridge”, relying on visual object grounding [27, 33] to know if it has reached its goal. This task is useful for household and assistive robot activities that may need to find and manipulate target objects in novel scenes [24, 54]. Although ObjectNav has been well studied in *static* environments [17, 19, 45, 46], its adoption

to dynamic real-world scenarios, where humans move target objects over time, is yet to be investigated.

Performing embodied navigation in dynamic environments is relevant in household scenarios involving finding small, portable objects a user tends to move around. For instance, if a user routinely leaves their car keys in the garage during the afternoon but has them in the kitchen at night, an agent tasked with finding the keys needs to estimate not just *where* they are, but also *when* the keys are potentially that location. In many cases, a human may also need to gather multiple portable items, such as a phone, wallet, and keys, when leaving the house. Analogous to Chatbots that provide personalized textual assistance based on historical data [26], embodied agents deployed in houses must learn from user behaviors to personalize their actions. Object transit routes are governed by user behaviors or habits [59, 60], and learning these transit behaviors would allow embodied agents to adapt better to human-centric environments and provide personalized assistance.

In this paper, we generalize ObjectNav to dynamic scenarios by formulating the *Portable Object Navigation* or *P-ObjectNav* task. P-ObjectNav assumes a non-static environment, requiring an embodied agent to be in the right place, at the right time for it to “capture” a shifting target. ObjectNav thus becomes a special case of P-ObjectNav, where target objects remain stationary throughout the epoch.

A key motivation for P-ObjectNav stems from the limitations of applying ObjectNav policies in dynamic settings common in the real world: agents must account for an evolving scene, where target objects such as a mug may be in the kitchen in the morning but move to the living room by the afternoon. This shift requires the agent to develop a time-sensitive navigation policy that can adapt to changing locations.

Current learning-based techniques for ObjectNav often involve Reinforcement Learning [4, 58, 61], where agents navigate using learned knowledge about fixed target positions from various sensor readings in different scenes. LLM-based zero-shot methods [6, 17, 53] have also been introduced, utilizing commonsense knowledge on target object positions (mug likely in kitchen) in their policies. These

\*Equal contribution.

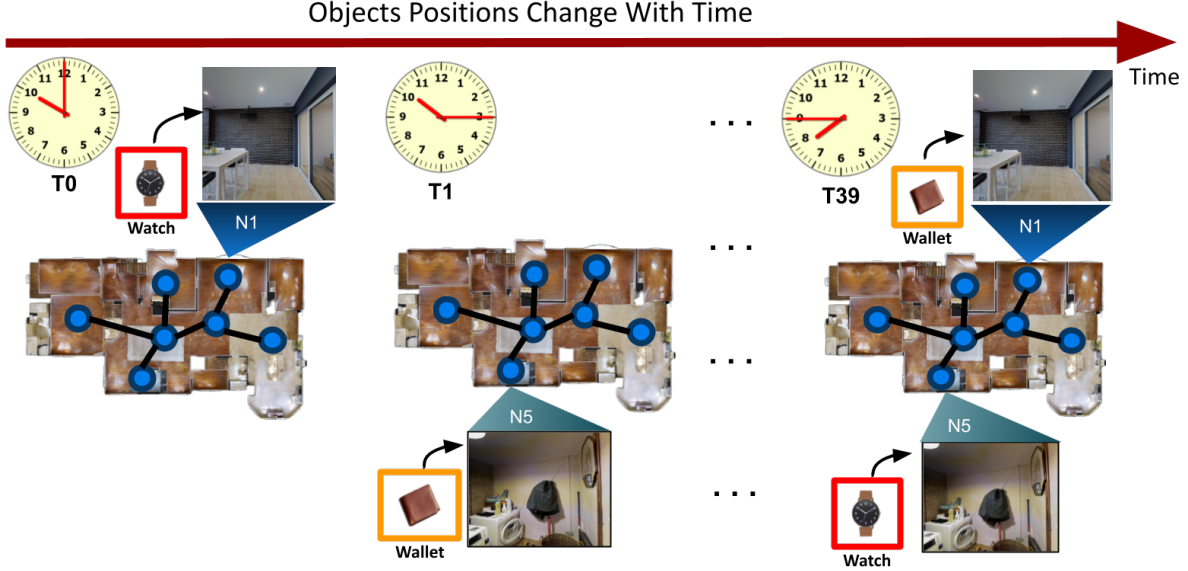


Figure 1. **Portable ObjectNav**: We generalize the task of ObjectNav to dynamic environments with portable targets. In this representative figure, the watch (in red) moves from node  $N1$  at  $T=10:00$  AM to node  $N5$  at  $T=7:45$  PM, while the wallet (in orange) moves from node  $N5$  at  $T=10:15$  AM to node  $N1$  at  $T=7:45$  PM. In our work, we study the performance of various navigation agents in different object transition scenarios, hypothesizing that a routine or structure in object transit is necessary to make the task of finding portable targets feasible.

stationary-target approaches must be able capture the dynamic nature of the environment to improve performance.

Traditionally, navigation in dynamic environments has focused on *low-level* planning tasks, like crowd avoidance [5, 36, 48] and socially aware navigation [7, 34], where agents continuously maneuver to avoid obstacles while minimizing trajectory length or time. By contrast, *high-level* planning tasks, such as ObjectNav and embodied exploration, are usually performed in static settings, focusing on sequential decision-making at nodes in a topological graph [9, 52]. With P-ObjectNav, we extend high-level planning to dynamic scenes with shifting targets by introducing dynamic topological graphs. While recent simulators like Habitat 3.0 [40] include rearrangement tasks where agents collaborate to move objects, our task is rather about finding shifting targets.

The dynamic nature of P-ObjectNav fundamentally challenges the static-scene assumption of ObjectNav, and helps bridge the gap towards finding targets in the real world. Our work lays the foundation for this by introducing strategies to dynamize existing scene graphs, setting a navigation benchmark with existing approaches, as well as introducing novel evaluation metrics to measure performance.

**Main Results.** We aim to foster research on *dynamic* embodied navigation by 1) formally defining a task involving finding non-stationary objects and 2) providing a general approach for dynamizing static scenes. Our contributions are summarized as follows:

- **Novel Task Setup:** We develop a novel formulation that generalizes ObjectNav to scenes with non-stationary or

portable objects. We refer to this task as *Portable ObjectNav* or *P-ObjectNav*. A P-ObjectNav agent aims to collect all possible portable objects in a scene over a fixed time period.

- **Routine Hypothesis:** If objects move randomly without a predictable structure, a learning agent’s performance may not improve over time. We use this observation to formulate a hypothesis for P-ObjectNav, postulating that over time, the performance of an agent under *routine* object transition must surpass that of *random* transition.
- **Dynamizing Scene Graphs:** We develop a novel approach for making static scene graphs dynamic, by placing and moving small portable objects in the scene. For this, we introduce three **object transition styles** for that govern the movement of objects. Our method applies to any topological scene graph, including those provided by Matterport3D (MP3D) [8] and HM3D [42]. We will release our dynamized MP3D environments and code as an open-source benchmark to foster research in this area.
- **Establishing P-ObjectNav Benchmark:** We establish a benchmark for the P-ObjectNav task by deploying heuristic, RL, and LLM-based agents in the various object placement scenarios. Further, we introduce three **novel evaluation metrics** to measure the performance of P-ObjectNav agents: *Object Finding Rate (OFR)*, *Cumulative Objects Found (COF)*, and *Trajectory Alignment (TA)* that give us insight into agent performance. Using these metrics, we report some interesting observations on the effects of memory and transit styles on P-ObjectNav performance.

## 2. Related Works

### 2.1. Object Navigation

Recent developments in Embodied Simulators [8, 14, 40, 42, 50] and subsequent works [4, 6, 29, 43, 46, 63] have established ObjectNav as a popular task in the computer vision field. These also include zero-shot approaches that employ various foundation models [17–19, 39, 69]. However, ObjectNav has predominantly been done in static environments, with fixed targets. While Habitat 3.0 [40] introduces the Social Rearrangement task, this is a human-robot teaming task where the agent is expected to rearrange objects in the house in tandem with the human. Our work deals strictly with the case where the agent is expected to find a non-stationary target without human assistance.

### 2.2. Exploration in Dynamic Environments

Planning in dynamic environments has been studied in the past [37, 55, 70], with recent approaches even utilizing LLMs in conjunction with multi-arm bandits [13]. These schemes usually propose memory augmentations with hierarchical planning procedures and frame the problem from an obstacle avoidance standpoint [28, 55, 67]. In contrast, our work considers the case where the objects themselves are non-stationary.

Rudra et al. [47] define small portable objects around the house, and propose a contextual bandit scheme that aims to learn the likelihood of finding an object at various waypoints. In their case, however, object locations are shuffled only after each epoch, meaning it finally boils down to an ObjectNav task in a static environment. In contrast, we tackle a *truly* dynamic case, where objects are moving even *during* the epoch. This definition adds a layer of complexity as the embodied agent must now navigate towards a constantly shifting target object, for which it needs to identify specific routines and object movement patterns in the environment.

Kurenkov et al. [25] introduced dynamizing household environments and experimented with scene graph memory to predict object locations. They also perform target object finding experiments, but the environment was static as the agent moved. In our work, the objects move as the agent moves. Furthermore, Wang et al. [56] used LLM-generated human activities to dynamize a scene graph of a household environment and performed ObjectNav experiments in these environments. In contrast, our work generalizes to generating dynamic environments from any topological graph and focuses on introducing the formulation, metrics, and benchmarks for P-ObjectNav.

### 2.3. Visual-Language Grounding

An important component of ObjectNav is the object detection module that allows the embodied agent to per-

ceive and understand the household scene. Object detection and semantic segmentation datasets like MS-COCO [30], ImageNet-2K [15], and LVIS [21] have brought great strides in pre-training visual models for everyday items. Furthermore, recent developments in vision foundation models [23, 27, 66] have allowed for zero-shot object detection and segmentation in household environments. With the advent of LLMs, a lot of new approaches for Object Navigation, especially in zero-shot conditions [16, 17, 19, 20, 64, 68] that rely solely on commonsense knowledge or LLM planning capabilities have garnered much interest. In our work, we adopt one of these approaches, LGX, and enhance it with memory to set a benchmark for P-ObjectNav.

## 3. P-ObjectNav: Task Overview

In this section, we formally define the P-ObjectNav task and establish our hypothesis for its optimal performance.

### 3.1. P-ObjectNav Definition

ObjectNav is defined in literature [4] as finding and grounding a target object specified by a target label in a previously unseen environment. Prior techniques [17, 19, 61] for solving this can be broadly broken down into two components 1) Sequential Decision Making and 2) Visual Grounding. The latter decides how the agent should navigate at each waypoint, while the former decides where the target object lies in the final image. Our work introduces **two key changes** to this setup -

1. We introduce temporal dynamism to the static embodied environment by adding transitory *portable* objects, and spatial dynamism by placing them at various parts of the scene.
2. There is no singular intended target per epoch (“Get to the chair”, for example), but rather the task is to find as many portable targets as possible within the epoch.

ObjectNav can be treated as a special case of P-ObjectNav when the target objects remain in one location and orientation in the scene throughout an epoch.

Let  $\Lambda$  describe the transitory motions of objects. Then, let  $O$  be the set of portable objects found over  $T$  timesteps for an agent starting at node  $r$  with an object distribution density  $d$ . Then  $S = [r, d, T, \Lambda]$  represents a set of our experimental variables for this task.

We can then define the objective of P-ObjectNav as “*Finding and visually grounding the **maximum** number of portable objects  $O$  while traversing a dynamic environment represented by  $S$ .*”. We study the performance of different navigation policies with varying simulator conditions  $S$ . A mathematical formulation for this is developed in this next subsection.

### 3.2. P-ObjectNav Problem Formulation

P-ObjectNav tackles ObjectNav in a constantly changing dynamic environment, with non-stationary target objects. This setting introduces a unique challenge for the agent that needs to be at the right place, at the right time to successfully ground a target object. In each epoch, the agent is tasked with finding as many portable target objects as it can. We consider this to be a high-level graph planning problem, requiring the agent to make decisions at nodes on a topological graph  $G$ . For this high-level navigation problem, define a finite trajectory  $\tau$  as a sequential list of visited nodes on  $G$ . Let  $\tau(t)$  be the  $t$ -th node in  $\tau$  and the value  $O(\tau(t))$  represent the set of portable targets found at node  $\tau(t)$  during timestep  $t$ . Given a trajectory  $\tau$  of length  $T$ , we can formulate the set of portable objects found  $O_\tau$  as,

$$O_\tau = \cup_{t=1}^T O(\tau(t)). \quad (1)$$

An agent parameterized by navigation policy  $\pi$  must generate a trajectory  $\tau_\pi$ . We now can write the policy optimization problem as finding an optimal policy  $\pi^*$  defined as,

$$\pi^* = \arg \max_{\pi} |O_\pi|, \quad (2)$$

where  $O_\pi$  is the set of portable objects found by  $\tau_\pi$ . Consequently,  $O_{\pi^*}$  is the maximum number of portable targets that can be found by taking the optimal trajectory. Given that the scene is dynamic, there is a chance for  $O_\pi = \emptyset$ . In the next section, we hypothesize a scenario that could improve the performance of a P-ObjectNav agent over time.

### 3.3. Routine Hypothesis

While the object positions are non-stationary, we hypothesize that the *object routes* need to be constant for an agent to learn patterns for successful task completion. We consider this consistency in object routes to be representative of human habits as routines [12].

Since the number of possible trajectories is finite on the undirected graph  $G$  given a time constraint  $T$ , a  $\pi^*$  that maximizes the number of portable objects collected must be attainable. We hypothesize that when objects are placed according to a fixed *routine* on  $G$ , as the ground truth portable object trajectory  $\tau^*$  remains constant, an optimal policy  $\pi^*$  is learnable over a set of epochs. Conversely, if objects are moved at *random* without any underlying pattern,  $\tau^*$  would change for each epoch, i.e., maximizing the variance of object placement in  $G$ . This scenario nullifies the agent's ability to learn beyond mere chance. As such, to prove our routine hypothesis, we need to experimentally show that,

$$\lim_{T \rightarrow \infty} (\mathcal{P}_{routine}(T) - \mathcal{P}_{random}(T)) \gg 0, \quad (3)$$

where  $\mathcal{P}_{routine}$  represents the agent's performance in a routine following environment, and  $\mathcal{P}_{random}$  represents performance when P-Object motions are random. Over time, a P-ObjectNav agent in an environment with object transit styles following a structure or routine should outperform an agent placed in a random environment. We describe our object transit schemes in the following section.

---

#### Algorithm 1 Modify Graph With Object Transitions $\Lambda$

---

**Input:** Topological Graph Environment  $G$  with set of vertices  $V$ , Portable Object Set  $O$ , Epoch Length  $T$ , Initial Agent Node  $r$ , Object Density  $d$ , Object Transit Scenario  $\Lambda$  (Equation 4), Local Graph Size  $q$ .

**Output:** Evolving Graph Trajectory  $\zeta$

**Initialize:** Add  $O$  portable objects to  $G_0$ , according to  $\Lambda$ . Calculate the object density  $d$  of the local graph  $g$  around the initial node  $r$ .  $g$  is all nodes within  $q$  steps of  $r$ . Sample  $N \in O$  new objects and add them to random nodes in  $g$  to match required density  $d$ .  $O' = O + N$  is the total set of objects at  $G_0$

- 1: **for**  $t \in [1, \dots, T]$  **do**
  - 2:    $G_t = G_{t-1}$
  - 3:   Sample  $k$  new vertices from  $V$  for each object  $o \in O'$  according to  $\Lambda$
  - 4:   Note:  $k$  could also be the same vertex, meaning the object does not move
  - 5:   Compute a path  $\delta(t)$  from the current vertex of the object  $v_o$  to its new vertex  $v_k$
  - 6:   Move  $o$  along  $\delta$  to its new location  $v_k$  over  $t$  timesteps
  - 7:   Add  $G_t$  to  $\zeta$
  - 8: **end for**
  - 9: **return**  $\zeta$
- 

## 4. Dynamizing Static Scene Graphs

To setup P-ObjectNav, we first introduce an approach to modify a topological scene graph with *temporal* and *spatial* object placements as follows:

### 4.1. Object Transitions

We consider three Object Transition Scenarios to induce non-stationary movement: **Random**, **Semi-Routine** and **Fully-Routine**. These are described in Table 2. Our routine hypothesis described in the previous section requires us to show that a learning-based agent's performance under a structured object transit scenario (semi-routine and routine) must outperform its performance in a random object transit scenario.

Algorithm 1 describes our approach for generating an graph trajectory  $\zeta$  to dynamize any given topological graph  $G$ . Figure 2 further illustrates this setup. The initial graph contains portable objects placed according to Table 1. We

Room	Portable Objects
Bedroom	Charger, Water Bottle, Smartwatch, Laptop, Notebook, Toothbrush, Mug, USB Flash Drive, Phone, Headphones, Hat
Garage	Screwdriver, Flashlight, Mug, Phone, Headphones, Hat
Dining	Salt and Pepper Shakers, Portable Speaker, Charger, Water Bottle, Mug, Bowl, Phone, Headphones, Hat
Office	Charger, Laptop, Hat, Notebook, USB Flash Drive, Mug, Phone, Headphones
Bathroom	Toothbrush, Phone, First-Aid Kit
Kitchen	Salt and Pepper Shakers, Hat, Mug, Bowl, Phone, Headphones, First-Aid Kit
Lounge	Playing Cards, Mug, Portable Speaker, Charger, Water Bottle, Laptop, Phone, USB Flash Drive, Dice, Headphones, Hat
Gym	Dumbbells, Jump rope, Smartwatch, Phone, Headphones, Hat
Outdoor	Jump rope, Smartwatch, Portable Speaker, Phone, Water Bottle, Headphones, Hat
Recreation	Playing Cards, Dice, Water Bottle, Headphones, Hat

Table 1. **Rooms and Portable Objects:** We map 21 portable objects to a set of rooms available in our Matterport3D scans. This mapping is used to set object locations during our Routine-based movement schemes. During each epoch, the objects are placed in different rooms during for a range of timesteps. Commonly moved objects such as *phone*, *headphones*, *hat* are associated with 9 different rooms, while less commonly shifted ones such as *dumbbells* appear only in the Gym.

### Object Transit: *Mug* from *Kitchen* to *Bedroom* at Timestep 53

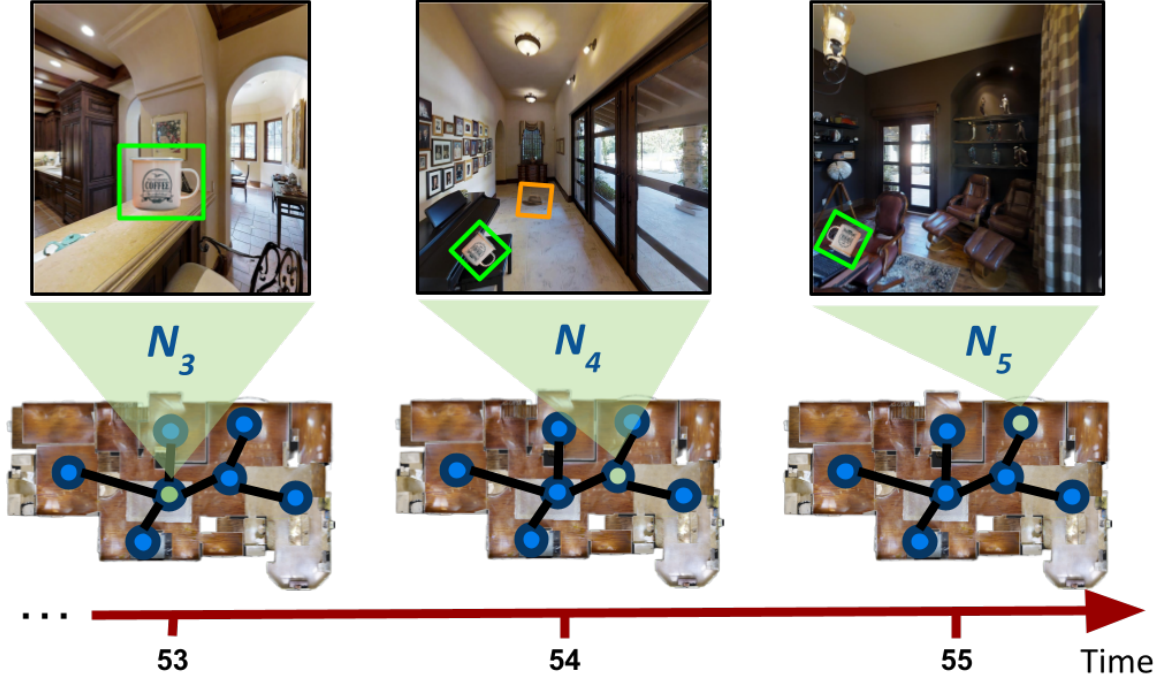


Figure 2. **Object Transition:** Portable objects move around the scene at various timesteps in accordance to their natural rooms (Table 1) and Transit Scenarios 2. Here, a *mug* is placed on a kitchen node  $N_3$  at timestep  $T = 53$ , but moves to a bedroom node  $N_5$  at timestep  $T = 55$  via node  $N_4$ . If an agent reaches the kitchen after  $T = 53$  (or the bedroom before  $T = 55$ ), it would fail to see the mug. Multiple objects could also be at the same node (note the hat marked in orange at  $N_4$ ). The varying orientations and sizes of the portable objects against different backgrounds makes small target grounding challenging; we tackle this as a separate problem in the Appendix.

then generate evolving graphs  $\zeta$  by moving objects in the graph at various timesteps for each transit scenario.  $\zeta$  is precomputed for each transit scenario and stored for later analysis with navigation algorithms.

When generating the evolving graph, a pseudo-random seed  $s$  helps differentiate the movement of portable objects

per epoch. Letting  $e$  be the epoch index,

$$s = \begin{cases} 1 \text{ (or fixed)} & \text{if movement is fully routine,} \\ e & \text{if movement is random or semi-routine.} \end{cases} \quad (4)$$

Note that for the fully routine case,  $\zeta$  remains constant for all epochs of the experiment, meaning that the object

Transit Scenario ( $\Lambda$ )	Fixed Rooms	Fixed Paths
Stationary (ObjectNav)	✓	N/A
Random	✗	✗
Semi-Routine	✓	✗
Fully-Routine	✓	✓

Table 2. **Object Transit Scenarios  $\Lambda$** : Different cases for portable object movement. In the random case, the portable objects can move to any room at any time during each epoch. In the routine cases, the rooms that the target objects can belong to are fixed (Table 1), except for when in transit. The stationary scenario emulates ObjectNav, where targets are stationary and do not move.

transition routes remain fixed. In the other two cases,  $\zeta$  varies per epoch according to the room and interval variability described.

We modify the Matterport3D (MP3D) [8] dataset which provides a topological graph of various household environments for our experiments. MP3D provides us with a topological graph with each node containing panoramic images representing images of the scene, and edges representing the distance between them. Additionally, each node contains information about the room type. We use these room types to define the set of portable objects listed in Table 1.

A successful P-ObjectNav agent on MP3D must determine the right sequence of discrete node “hops” to maximize object finding capability, for which it must learn the underlying object transit patterns.

## 4.2. Spatial Placement

Beyond object transitions, we also introduce spatial transformations in placing the objects on the scene. Portable objects are small and can be pasted on the scene in a variety of ways.

We first use FastSAM [65] to obtain segmentation masks for both the scene and the portable target object. On the scene segmentations, we filter out a set of  $K$  largest segments below the center of the image, to avoid placing floating targets. We then place the target objects on a randomly chosen segment  $k \in K$  this set. While 3D object placement would be more accurate, it is also far more cumbersome, requiring access to a simulator. This simple placement technique for small objects allows us to modify images of pre-existing topological graphs and makes the visual grounding task challenging enough for comparison against various backgrounds. More details on our visual grounding experiments with VLMs can be found in the Appendix. We will be releasing this dataset of small objects placed on MP3D to foster research in embodied visual grounding.

## 5. P-ObjectNav Policies

For a fair comparison with prior work, we emulate the static environment of ObjectNav by keeping portable objects stationary in one location throughout the experiment. We then

evaluate both the static ObjectNav environment and the dynamic P-ObjectNav environment with three relevant SOTA navigation agents from current literature.

### 5.1. Oracle Agent

We utilize a greedy heuristic on an agent as an oracle baseline: At each timestep  $t \in [1, T - 1]$ , we perform a Breadth-First Search (BFS) to find the closest node with an unseen portable object. The agent then moves to a neighboring node in the direction of this object. This approach relies on the agent having access to an “oracle” which tells it about the closest node containing a unique portable target at a given timestep. While oracle knowledge is useful, since the position of the objects in the environment change with time, note that there is a possibility that it will not find an object after navigating to an oracle-guided node.

### 5.2. Reinforcement Learning Agent

We use a reinforcement learning-based method, specifically Proximal Policy Optimization (PPO) [51] to define a P-ObjectNav agent. PPO has been used in several previous works that tackled embodied navigation tasks, including ObjectNav [57, 61, 71] with SOTA results. Given the limited prior literature dealing with PPO on a dynamic scene graph, we consider constructing our own agent with the following observation space:

- Current timestep,  $t \in T$
- Index of the current node,  $n_t$  from a list of all nodes in the environment graph
- A list with each index corresponding to a node, and the element at a given index being the number of objects at the corresponding node at  $t$
- Another list with each index corresponding to a node. The element at a given index is 1 if the corresponding node is an immediate neighbor to the current node and 0 otherwise.

The PPO agent then outputs the index of the node it wants to travel to for the next timestep  $t + 1$ . Let  $O_{t-1}$  be the set of distinct portable objects the agent has seen up to time  $t - 1$ . The reward is the number of new objects it has found at the current node  $n_t$  that are not in  $O_{t-1}$ . Formally the reward at timestep  $t$  is  $|O(n_t) \setminus O_{t-1}|$ . We also note that this structure requires access to a map of the environment and oracle knowledge of the number of new objects at each node at each timestep.

### 5.3. LLM-based Agents

For LLM-based navigation, we consider two variations of LGX [17], an LLM-based SOTA for zero-shot ObjectNav.

**LGX-Vanilla**: Given a target object, the vanilla version of LGX takes a list of objects around the agent and asks an LLM (GPT-4o) to predict an object to navigate toward. The agent then navigates towards the predicted object, and continues doing so till the provided target is found.

Since our task definition requires the agent to find all portable targets, we replace the target object in LGX’s prompt with a set of portable targets remaining to be found in the environment. At each timestep, we use YOLO v8 [22] to obtain a list of objects in the scene, and then prompt GPT-4o with the object list asking for an object prediction from the list that might lead to an unseen portable object. We then use the MP3D scene graph to hop to the next node.

**LGX-Memory:** The vanilla version of LGX works in a zero-shot manner resembling a Markov chain, meaning that it makes navigation decisions at each node solely based on the observations it has seen at the current timestep. Since objects keep transiting on our dynamic scene graph, keeping track of previously seen objects should help the agent make more prudent navigational decisions.

We accommodate this by incorporating LGX with memory by passing a set of historical objects seen, predictions made, and timesteps to the prompt across epochs. The system prompt contains this historical data, along with a set of portable objects remaining to be found in the environment. We maintain a horizon to avoid GPT token overflow, where we remove the earliest appended observation when an overflow of tokens occurs.

## 6. Experiments and Results

We treat navigating in dynamic scenes and visual target grounding as separate problems in our experiments. This decoupling allows us individually analyze navigation and grounding performance. Results of our visual grounding task are explained in detail in the supplementary.

### 6.1. Hyperparameters

We determine 4 hyperparameters that influence performance as described in the definition section, i.e.,  $S = [r, d, T, \Lambda]$ . Each agent is subjected to a total of  $[Stationary(1) + Transit(3)] \times R \times E \times T$  experiments, where  $R$  is a set of rooms that varies with each scan from which a random node  $r \in R$  is picked as a starting point for each trial. The maximum number of trials is thus equal to the number of rooms.  $R$  ranges from [11, 30] in our chosen subset of 10 MP3D scans.  $E$  is the number of epochs that we run for each starting node  $r$ , and  $T$  is the number of timesteps per epoch. We set  $R = 10$ ,  $E = 10$  and  $T = 30$  in our experiments.

**Ground Truth Path ( $\pi^*$ ):** Given a starting node  $r \in R$ , for each epoch  $e \in E$ , there exists a set of ground truth paths over  $T$  that the agent could take for collecting the most number of portable targets. We compute these paths by simulating all possible trajectories from a given starting point  $r$ , and store it to calculate trajectory efficiencies later.

**Object Density:** We perform ablations with varying the density of portable objects in a scan. Object density is defined as  $d = \text{Num. Portable Objects} / \text{Graph Size}$ , and is

one of our simulation parameters.

### 6.2. Evaluation Metrics

Since we introduce a new task, we also define 3 new metrics to evaluate it. All metrics are averaged out across each scan. The equations for these are in Table 3. These are:-

- **Cumulative Objects Found (COF):** This is the maximum number of *unique* portable targets found across all epochs averaged across starting nodes  $r$ . This value gives us an estimate of the absolute best performing agents.
- **Object Finding Rate (OFR)** is analogous to the Success Rate (SR) metric used in ObjectNav [2] and represents the average success in finding portable objects across rooms.
- **Trajectory Alignment (TA):** This is a path efficiency metric similar to the SPL metric popular in ObjectNav evaluation [2]. We define this as the overlap between the GT trajectory ( $\tau^*$ ) and the trajectory taken by the agent ( $\tau$ ) across all epochs and starting nodes.

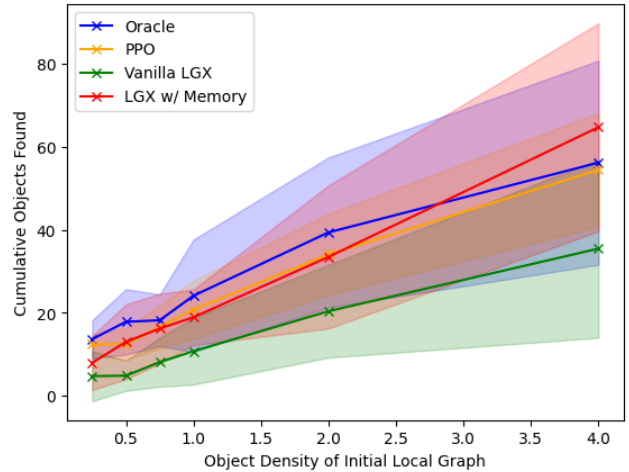


**Figure 3. COF vs OD:** We ablate our approaches over multiple object densities. This plot shows all objects found over. Observe that the rising trend, with the LGX + Memory approach outperforming even the supervised Oracle at high density.

### 6.3. Navigation Inference

Table 3 presents the results of our agents on the P-ObjectNav task. We run experiments on 10 Matterport3D scans, with 10 randomly selected starting nodes  $r \in R$ , 20 epochs and each epoch having 20 timesteps.

**Memory Improves Performance, But Only Slightly:** When comparing the OFR values between the Vanilla LGX and LGX + Memory approaches, note the improved performance of the former. The agent’s memory or system prompt at each epoch contains the entire history of actions that it took on all timesteps in all epochs before it. As such, there should be an improvement in performance with increasing epochs. While we notice this improvement with increasing density (Fig. 3), the OFR, which averages success over

Policy	Object Transit	P-ObjectNav		
		COF $\uparrow$	OFR (%) $\uparrow$	TA (%) $\uparrow$
Oracle Agent	Stationary (ObjectNav)	8.77 $\pm$ 1.56	<b>90.19 <math>\pm</math> 6.55</b>	45.6 $\pm$ 7.80
	Random	<b>10.64 <math>\pm</math> 3.62</b>	78.43 $\pm$ 6.32	<b>54.40 <math>\pm</math> 9.05</b>
	Semi-Routine	8.81 $\pm$ 2.07	75.08 $\pm$ 6.33	50.58 $\pm$ 6.01
	Fully-Routine	7.00 $\pm$ 1.89	58.88 $\pm$ 7.26	32.68 $\pm$ 5.12
PPO Agent	Stationary (ObjectNav)	5.66 $\pm$ 0.98	<b>59.09 <math>\pm</math> 9.40</b>	<b>41.60 <math>\pm</math> 8.60</b>
	Random	<b>7.15 <math>\pm</math> 1.65</b>	55.20 $\pm$ 5.92	37.33 $\pm$ 4.95
	Semi-Routine	6.87 $\pm$ 1.38	57.75 $\pm$ 7.84	35.79 $\pm$ 5.64
	Fully-Routine	6.55 $\pm$ 1.62	55.15 $\pm$ 7.67	32.06 $\pm$ 4.68
Vanilla LGX	Stationary (ObjectNav)	2.68 $\pm$ 0.51	28.51 $\pm$ 8.73	24.33 $\pm$ 5.40
	Random	5.59 $\pm$ 1.47	43.28 $\pm$ 12.05	30.74 $\pm$ 8.69
	Semi-Routine	<b>5.64 <math>\pm</math> 1.06</b>	<b>47.23 <math>\pm</math> 8.03</b>	<b>31.3 <math>\pm</math> 5.14</b>
	Fully-Routine	3.95 $\pm$ 0.68	34.23 $\pm$ 8.58	21.70 $\pm$ 5.42
LGX + Memory	Stationary (ObjectNav)	4.74 $\pm$ 0.87	50.63 $\pm$ 14.85	<b>36.94 <math>\pm</math> 8.36</b>
	Random	6.19 $\pm$ 0.79	49.43 $\pm$ 11.41	33.79 $\pm$ 8.81
	Semi-Routine	<b>6.30 <math>\pm</math> 1.22</b>	<b>53.20 <math>\pm</math> 6.70</b>	34.62 $\pm$ 5.57
	Fully-Routine	5.71 $\pm$ 1.34	47.88 $\pm$ 7.82	32.42 $\pm$ 3.86

## Metrics

$$\text{COF} = \frac{1}{R} \sum_{r \in R} \max_{e \in E} O_\tau$$

$$\text{OFR} = \frac{1}{R} \sum_{r \in R} \max_{e \in E} \frac{O_\tau}{O_{\tau^*}}$$

$$TA = \frac{1}{R \cdot E} \sum_{r \in R} \sum_{e \in E} \frac{\tau}{\tau^*}$$

**Table 3. P-ObjectNav Metrics and Results:** We evaluate 4 popular embodied navigation policies on various Object Transit scenarios for P-ObjectNav. Highlighted in blue are transit cases with shifting objects. Our metrics are defined on the right. Note the superior performance of the Oracle Agent across all metrics. Also note the improved performance of LGX when it is augmented with memory.

ground truth across all starting nodes and scans shows only a minor improvement of 8.59% on average across cases of object transit (in blue). The absence of a large improvement despite knowing which actions did not lead to a portable target may be attributed to the overloading of memory on GPT-4o, or that LGX does not directly utilize visual embeddings in its outcome. We investigate this further in the Appendix.

**ObjectNav vs. P-ObjectNav:** On the Oracle and PPO agents, note the improved OFR performance of agents in the stationary transit case intended to mimic ObjectNav. Both these agents use supervision of some form, despite which P-ObjectNav performs poorly in comparison, highlighting the challenging nature of this task. On the Vanilla LGX policy which is zero-shot, we note a dip in performance in the stationary case. Upon further inspection, we notice that this agent often tends to oscillate between two nodes, due to which it fails to find most target objects. More details about this are in the Appendix.

**Routine Hypothesis Holds True, To Some Extent:** The hypothesis that we set up in our formulation section was that an agent in routine-following dynamic environments would outperform those in a random transit scenario. This holds true on the PPO and LGX agents, but slightly fails with the Oracle agent. Further, the best performance seems to be with the semi-routine case with the LLM-based approaches. This is an interesting result that could be attributed to agents performing best when environments are not too strictly structured. For instance, there are often cases when an agent misses an object despite being in the right room, as the object’s transitory path was too strict and did not deviate in between epochs. We discuss more details,

graphs and inferences in the Appendix.

## 7. Conclusion, Limitations, and Further Work

We present and lay the foundation for P-ObjectNav, a generalization of the ObjectNav task in dynamic environments with shifting objects. Unlike ObjectNav where an agent is expected to navigate to *stationary* target objects, P-ObjectNav is more realistic and challenging, in introducing portability among target objects in the scene. The dynamic nature of our task fundamentally challenges the static-scene assumption common in ObjectNav literature.

In setting up P-ObjectNav, we introduce a novel approach to dynamize scene graphs with various object transition styles, and placing small targets against various backgrounds. Our approach can be used to dynamize any topological scene graph such as MP3D. Further, we hypothesize that routine-following object transition should increase navigation success, and support this claim via evaluation with novel metrics designed for our task. Code and data for P-ObjectNav, including the dynamized MP3D dataset will be made publicly available to foster research in this exciting new direction of embodied navigation in dynamic scenes.

A limitation of our current approach is that we independently evaluate navigation and visual grounding. As such, errors in the navigation stage would not influence the grounding and vice versa. Coupling these experiments for a real-world deployment to finding portable targets by learning object transition habits is a future direction. Another interesting direction is to combine generative image modeling with 2D simulators such as Minigrad [11], which would allow us to scale up experimentation and training.

## References

- [1] Josh Achiam, Steven Adler, Sandhini Agarwal, Lama Ahmad, Ilge Akkaya, Florencia Leoni Aleman, Diogo Almeida, Janko Altenschmidt, Sam Altman, Shyamal Anadkat, et al. Gpt-4 technical report. *arXiv preprint arXiv:2303.08774*, 2023. 2
- [2] Peter Anderson, Angel Chang, Devendra Singh Chaplot, Alexey Dosovitskiy, Saurabh Gupta, Vladlen Koltun, Jana Kosecka, Jitendra Malik, Roozbeh Mottaghi, Manolis Savva, et al. On evaluation of embodied navigation agents. *arXiv preprint arXiv:1807.06757*, 2018. 7
- [3] Peter Anderson, Qi Wu, Damien Teney, Jake Bruce, Mark Johnson, Niko Sünderhauf, Ian Reid, Stephen Gould, and Anton Van Den Hengel. Vision-and-language navigation: Interpreting visually-grounded navigation instructions in real environments. In *Proceedings of the IEEE conference on computer vision and pattern recognition*, pages 3674–3683, 2018. 1
- [4] Dhruv Batra, Aaron Gokaslan, Aniruddha Kembhavi, Oleksandr Maksymets, Roozbeh Mottaghi, Manolis Savva, Alexander Toshev, and Erik Wijmans. Objectnav revisited: On evaluation of embodied agents navigating to objects. *arXiv preprint arXiv:2006.13171*, 2020. 1, 3
- [5] Kuanqi Cai, Chaoqun Wang, Jiyu Cheng, Clarence W De Silva, and Max Q-H Meng. Mobile robot path planning in dynamic environments: A survey. *arXiv preprint arXiv:2006.14195*, 2020. 2
- [6] Tommaso Campari, Leonardo Lamanna, Paolo Traverso, Luciano Serafini, and Lamberto Ballan. Online learning of reusable abstract models for object goal navigation. In *Proceedings of the IEEE/CVF Conference on Computer Vision and Pattern Recognition*, pages 14870–14879, 2022. 1, 3
- [7] Enrico Cancelli, Tommaso Campari, Luciano Serafini, Angel X Chang, and Lamberto Ballan. Exploiting proximity-aware tasks for embodied social navigation. In *Proceedings of the IEEE/CVF International Conference on Computer Vision*, pages 10957–10967, 2023. 2
- [8] Angel Chang, Angela Dai, Thomas Funkhouser, Maciej Halber, Matthias Niessner, Manolis Savva, Shuran Song, Andy Zeng, and Yinda Zhang. Matterport3d: Learning from rgb-d data in indoor environments. *arXiv preprint arXiv:1709.06158*, 2017. 2, 3, 6
- [9] Kevin Chen, Junshen K Chen, Jo Chuang, Marynel Vázquez, and Silvio Savarese. Topological planning with transformers for vision-and-language navigation. In *Proceedings of the IEEE/CVF Conference on Computer Vision and Pattern Recognition*, pages 11276–11286, 2021. 2
- [10] Tianheng Cheng, Lin Song, Yixiao Ge, Wenyu Liu, Xinggang Wang, and Ying Shan. Yolo-world: Real-time open-vocabulary object detection, 2024. 2, 4
- [11] Maxime Chevalier-Boisvert, Bolun Dai, Mark Towers, Rodrigo de Lazcano, Lucas Willems, Salem Lahlou, Suman Pal, Pablo Samuel Castro, and Jordan Terry. Minigrid & miniworld: Modular & customizable reinforcement learning environments for goal-oriented tasks. *CoRR*, abs/2306.13831, 2023. 8
- [12] Florence Clark, Katherine Sanders, Michael Carlson, Erna Blanche, and Jeanne Jackson. Synthesis of habit theory. *OTJR: occupation, participation and health*, 27(1-suppl): 7S–23S, 2007. 4
- [13] J de Curtò, I de Zarzà, Gemma Roig, Juan Carlos Cano, Pietro Manzoni, and Carlos T Calafate. Llm-informed multi-armed bandit strategies for non-stationary environments. *Electronics*, 12(13):2814, 2023. 3
- [14] Matt Deitke, Eli VanderBilt, Alvaro Herrasti, Luca Weihs, Jordi Salvador, Kiana Ehsani, Winson Han, Eric Kolve, Ali Farhadi, Aniruddha Kembhavi, and Roozbeh Mottaghi. ProcTHOR: Large-Scale Embodied AI Using Procedural Generation, 2022. 3
- [15] Jia Deng, Wei Dong, Richard Socher, Li-Jia Li, Kai Li, and Li Fei-Fei. ImageNet: A large-scale hierarchical image database. In *2009 IEEE Conference on Computer Vision and Pattern Recognition*, pages 248–255, 2009. 3
- [16] Vishnu Sashank Dorbala, Gunnar A Sigurdsson, Jesse Thomason, Robinson Piramuthu, and Gaurav S Sukhatme. Clip-nav: Using clip for zero-shot vision-and-language navigation. In *Workshop on Language and Robotics at CoRL 2022*, 2022. 3
- [17] Vishnu Sashank Dorbala, James F Mullen Jr, and Dinesh Manocha. Can an embodied agent find your “cat-shaped mug”? Llm-based zero-shot object navigation. *IEEE Robotics and Automation Letters*, 2023. 1, 3, 6
- [18] Samir Yitzhak Gadre, Mitchell Wortsman, Gabriel Ilharco, Ludwig Schmidt, and Shuran Song. Clip on wheels: Zero-shot object navigation as object localization and exploration. *arXiv preprint arXiv:2203.10421*, 2022.
- [19] Samir Yitzhak Gadre, Mitchell Wortsman, Gabriel Ilharco, Ludwig Schmidt, and Shuran Song. Cows on pasture: Baselines and benchmarks for language-driven zero-shot object navigation. In *Proceedings of the IEEE/CVF Conference on Computer Vision and Pattern Recognition*, pages 23171–23181, 2023. 1, 3
- [20] Tianrui Guan, Yurou Yang, Harry Cheng, Muyuan Lin, Richard Kim, Rajasimman Madhivanan, Arnie Sen, and Dinesh Manocha. Loc-zson: Language-driven object-centric zero-shot object retrieval and navigation, 2023. 3
- [21] Agrim Gupta, Piotr Dollar, and Ross Girshick. Lvis: A dataset for large vocabulary instance segmentation. In *Proceedings of the IEEE/CVF Conference on Computer Vision and Pattern Recognition (CVPR)*, 2019. 3
- [22] Glenn Jocher, Ayush Chaurasia, and Jing Qiu. Ultralytics YOLO, 2023. 7
- [23] Alexander Kirillov, Eric Mintun, Nikhila Ravi, Hanzi Mao, Chloe Rolland, Laura Gustafson, Tete Xiao, Spencer Whitehead, Alexander C. Berg, Wan-Yen Lo, Piotr Dollár, and Ross Girshick. Segment anything, 2023. 3
- [24] Yuxuan Kuang, Hai Lin, and Meng Jiang. Openfm-nav: Towards open-set zero-shot object navigation via vision-language foundation models. *arXiv preprint arXiv:2402.10670*, 2024. 1
- [25] Andrey Kurenkov, Michael Lingelbach, Tanmay Agarwal, Emily Jin, Chengshu Li, Ruohan Zhang, Li Fei-Fei, Jiajun Wu, Silvio Savarese, and Roberto Martin-Martín. Modeling dynamic environments with scene graph memory. In *International Conference on Machine Learning*, pages 17976–17993. PMLR, 2023. 3

- [26] Lasha Labadze, Maya Grigolia, and Lela Machaidze. Role of ai chatbots in education: systematic literature review. *International Journal of Educational Technology in Higher Education*, 20(1):56, 2023. 1
- [27] Liunian Harold Li, Pengchuan Zhang, Haotian Zhang, Jianwei Yang, Chunyuan Li, Yiwu Zhong, Lijuan Wang, Lu Yuan, Lei Zhang, Jenq-Neng Hwang, Kai-Wei Chang, and Jianfeng Gao. Grounded Language-Image Pre-training, 2022. 1, 3, 2, 4
- [28] Weiyuan Li, Ruoxin Hong, Jiwei Shen, Liang Yuan, and Yue Lu. Transformer memory for interactive visual navigation in cluttered environments. *IEEE Robotics and Automation Letters*, 8(3):1731–1738, 2023. 3
- [29] Yiqing Liang, Boyuan Chen, and Shuran Song. Sscnav: Confidence-aware semantic scene completion for visual semantic navigation. In *2021 IEEE international conference on robotics and automation (ICRA)*, pages 13194–13200. IEEE, 2021. 3
- [30] Tsung-Yi Lin, Michael Maire, Serge J. Belongie, James Hays, Pietro Perona, Deva Ramanan, Piotr Dollár, and C. Lawrence Zitnick. Microsoft coco: Common objects in context. In *European Conference on Computer Vision*, 2014. 3
- [31] Haotian Liu, Chunyuan Li, Yuheng Li, and Yong Jae Lee. Improved baselines with visual instruction tuning. In *Proceedings of the IEEE/CVF Conference on Computer Vision and Pattern Recognition*, pages 26296–26306, 2024. 2
- [32] Haotian Liu, Chunyuan Li, Qingyang Wu, and Yong Jae Lee. Visual instruction tuning. *Advances in neural information processing systems*, 36, 2024. 2
- [33] Shilong Liu, Zhaoyang Zeng, Tianhe Ren, Feng Li, Hao Zhang, Jie Yang, Chunyuan Li, Jianwei Yang, Hang Su, Jun Zhu, et al. Grounding dino: Marrying dino with grounded pre-training for open-set object detection. *arXiv preprint arXiv:2303.05499*, 2023. 1
- [34] Christoforos I Mavrogiannis and Ross A Knepper. Decentralized multi-agent navigation planning with braids. In *Algorithmic Foundations of Robotics XII: Proceedings of the Twelfth Workshop on the Algorithmic Foundations of Robotics*, pages 880–895. Springer, 2020. 2
- [35] Matthias Minderer, Alexey Gritsenko, Austin Stone, Maxim Neumann, Dirk Weissenborn, Alexey Dosovitskiy, Aravindh Mahendran, Anurag Arnab, Mostafa Dehghani, Zhuoran Shen, Xiao Wang, Xiaohua Zhai, Thomas Kipf, and Neil Houlsby. Simple open-vocabulary object detection with vision transformers, 2022. 2, 4
- [36] M.G. Mohanan and Ambuja Salgoankar. A survey of robotic motion planning in dynamic environments. *Robotics and Autonomous Systems*, 100:171–185, 2018. 2
- [37] Timothy Morris, Feras Dayoub, Peter Corke, Gordon Wyeth, and Ben Ugcroft. Multiple map hypotheses for planning and navigating in non-stationary environments. In *2014 IEEE international conference on robotics and automation (ICRA)*, pages 2765–2770. IEEE, 2014. 3
- [38] Soroush Nasiriany, Fei Xia, Wenhao Yu, Ted Xiao, Jacky Liang, Ishita Dasgupta, Annie Xie, Danny Driess, Ayzaan Wahid, Zhuo Xu, et al. Pivot: Iterative visual prompting elicits actionable knowledge for vlms. *arXiv preprint arXiv:2402.07872*, 2024. 3
- [39] Bhrij Patel, Vishnu Sashank Dorbala, Amrit Singh Bedi, and Dinesh Manocha. Multi-llm qa with embodied exploration, 2024. 3
- [40] Xavier Puig, Eric Undersander, Andrew Szot, Mikael Dal-laire Cote, Tsung-Yen Yang, Ruslan Partsey, Ruta Desai, Alexander William Clegg, Michal Hlavac, So Yeon Min, et al. Habitat 3.0: A co-habitat for humans, avatars and robots. *arXiv preprint arXiv:2310.13724*, 2023. 2, 3
- [41] Yuankai Qi, Qi Wu, Peter Anderson, Xin Wang, William Yang Wang, Chunhua Shen, and Anton van den Hengel. REVERIE: Remote Embodied Visual Referring Expression in Real Indoor Environments, 2020. 1
- [42] Santhosh K Ramakrishnan, Aaron Gokaslan, Erik Wijmans, Oleksandr Maksymets, Alex Clegg, John Turner, Eric Undersander, Wojciech Galuba, Andrew Westbury, Angel X Chang, et al. Habitat-matterport 3d dataset (hm3d): 1000 large-scale 3d environments for embodied ai. *arXiv preprint arXiv:2109.08238*, 2021. 2, 3
- [43] Santhosh Kumar Ramakrishnan, Devendra Singh Chaplot, Ziad Al-Halah, Jitendra Malik, and Kristen Grauman. Poni: Potential functions for objectgoal navigation with interaction-free learning. In *Proceedings of the IEEE/CVF Conference on Computer Vision and Pattern Recognition*, pages 18890–18900, 2022. 3
- [44] Ram Ramrakhyia, Eric Undersander, Dhruv Batra, and Abhishek Das. Habitat-web: Learning embodied object-search strategies from human demonstrations at scale. In *Proceedings of the IEEE/CVF Conference on Computer Vision and Pattern Recognition*, pages 5173–5183, 2022. 1
- [45] Ram Ramrakhyia, Dhruv Batra, Erik Wijmans, and Abhishek Das. Pirlnav: Pretraining with imitation and rl finetuning for objectnav. In *Proceedings of the IEEE/CVF Conference on Computer Vision and Pattern Recognition*, pages 17896–17906, 2023. 1
- [46] Sonia Raychaudhuri, Tommaso Campari, Unnat Jain, Manolis Savva, and Angel X Chang. Mopa: Modular object navigation with pointgoal agents. In *Proceedings of the IEEE/CVF Winter Conference on Applications of Computer Vision*, pages 5763–5773, 2024. 1, 3
- [47] Sohan Rudra, Saksham Goel, Anirban Santara, Claudio Gentile, Laurent Perron, Fei Xia, Vikas Sindhwani, Carolina Parada, and Gaurav Aggarwal. A contextual bandit approach for learning to plan in environments with probabilistic goal configurations. In *2023 IEEE International Conference on Robotics and Automation (ICRA)*, pages 5645–5652. IEEE, 2023. 3
- [48] Adarsh Jagan Sathyamoorthy, Jing Liang, Utsav Patel, Tianrui Guan, Rohan Chandra, and Dinesh Manocha. Densecavod: Real-time navigation in dense crowds using anticipatory behaviors. In *2020 IEEE International Conference on Robotics and Automation (ICRA)*, pages 11345–11352. IEEE, 2020. 2
- [49] Adarsh Jagan Sathyamoorthy, Kasun Weerakoon, Mohamed Elnoor, Anuj Zore, Brian Ichter, Fei Xia, Jie Tan, Wenhao Yu, and Dinesh Manocha. Convoi: Context-aware naviga-

- tion using vision language models in outdoor and indoor environments. *arXiv preprint arXiv:2403.15637*, 2024. 2
- [50] Manolis Savva, Abhishek Kadian, Oleksandr Maksymets, Yili Zhao, Erik Wijmans, Bhavana Jain, Julian Straub, Jia Liu, Vladlen Koltun, Jitendra Malik, Devi Parikh, and Dhruv Batra. Habitat: A Platform for Embodied AI Research, 2019. 3
- [51] John Schulman, Filip Wolski, Prafulla Dhariwal, Alec Radford, and Oleg Klimov. Proximal policy optimization algorithms. *arXiv preprint arXiv:1707.06347*, 2017. 6
- [52] Dhruv Shah, Benjamin Eysenbach, Gregory Kahn, Nicholas Rhinehart, and Sergey Levine. Ving: Learning open-world navigation with visual goals. In *2021 IEEE International Conference on Robotics and Automation (ICRA)*, pages 13215–13222. IEEE, 2021. 2
- [53] Dhruv Shah, Blazej Osinski, Brian Ichter, and Sergey Levine. LM-Nav: Robotic Navigation with Large Pre-Trained Models of Language, Vision, and Action, 2022. 1
- [54] Jingwen Sun, Jing Wu, Ze Ji, and Yu-Kun Lai. A survey of object goal navigation. *IEEE Transactions on Automation Science and Engineering*, 2024. 1
- [55] Victor Vladareanu, Gabriela Tont, Luige Vladareanu, and Florentin Smarandache. The navigation of mobile robots in non-stationary and non-structured environments. *International Journal of Advanced Mechatronic Systems*, 5(4):232–242, 2013. 3
- [56] Chenxu Wang, Xinghang Li, Dunzheng Wang, Huaping Liu, et al. Dynamic scene generation for embodied navigation benchmark. In *RSS 2024 Workshop: Data Generation for Robotics*, 2024. 3
- [57] Erik Wijmans, Abhishek Kadian, Ari Morcos, Stefan Lee, Irfan Essa, Devi Parikh, Manolis Savva, and Dhruv Batra. Dd-ppo: Learning near-perfect pointgoal navigators from 2.5 billion frames. *arXiv preprint arXiv:1911.00357*, 2019. 6
- [58] Erik Wijmans, Abhishek Kadian, Ari Morcos, Stefan Lee, Irfan Essa, Devi Parikh, Manolis Savva, and Dhruv Batra. Dd-ppo: Learning near-perfect pointgoal navigators from 2.5 billion frames, 2020. 1
- [59] Wendy Wood and David T Neal. A new look at habits and the habit-goal interface. *Psychological review*, 114(4):843, 2007. 1
- [60] Wendy Wood and Dennis Runger. Psychology of habit. *Annual review of psychology*, 67(1):289–314, 2016. 1
- [61] Karmesh Yadav, Arjun Majumdar, Ram Ramrakhya, Naoki Yokoyama, Alexei Baevski, Zsolt Kira, Oleksandr Maksymets, and Dhruv Batra. Ovrl-v2: A simple state-of-art baseline for imagenav and objectnav. *arXiv preprint arXiv:2303.07798*, 2023. 1, 3, 6
- [62] Karmesh Yadav, Ram Ramrakhya, Santhosh Kumar Ramakrishnan, Theo Gervet, John Turner, Aaron Gokaslan, Noah Maestre, Angel Xuan Chang, Dhruv Batra, Manolis Savva, et al. Habitat-matterport 3d semantics dataset. In *Proceedings of the IEEE/CVF Conference on Computer Vision and Pattern Recognition*, pages 4927–4936, 2023. 1
- [63] Naoki Harrison Yokoyama, Sehoon Ha, Dhruv Batra, Jiguang Wang, and Bernadette Bucher. Vlfm: Vision-language frontier maps for zero-shot semantic navigation. In *2nd Workshop on Language and Robot Learning: Language as Grounding*, 2023. 3
- [64] Bangguo Yu, Hamidreza Kasaei, and Ming Cao. L3mvn: Leveraging large language models for visual target navigation. In *2023 IEEE/RSJ International Conference on Intelligent Robots and Systems (IROS)*. IEEE, 2023. 3
- [65] Xu Zhao, Wenchao Ding, Yongqi An, Yinglong Du, Tao Yu, Min Li, Ming Tang, and Jinqiao Wang. Fast segment anything. *arXiv preprint arXiv:2306.12156*, 2023. 6, 2
- [66] Xu Zhao, Wenchao Ding, Yongqi An, Yinglong Du, Tao Yu, Min Li, Ming Tang, and Jinqiao Wang. Fast segment anything, 2023. 3
- [67] Yan Zheng, Zhaopeng Meng, Jianye Hao, Zongzhang Zhang, Tianpei Yang, and Changjie Fan. A deep bayesian policy reuse approach against non-stationary agents. *Advances in neural information processing systems*, 31, 2018. 3
- [68] Gengze Zhou, Yicong Hong, and Qi Wu. Navgpt: Explicit reasoning in vision-and-language navigation with large language models, 2023. 3
- [69] Kaiwen Zhou, Kaizhi Zheng, Connor Pryor, Yilin Shen, Hongxia Jin, Lise Getoor, and Xin Eric Wang. Esc: Exploration with soft commonsense constraints for zero-shot object navigation. *arXiv preprint arXiv:2301.13166*, 2023. 3
- [70] Ye Zhou and Hann Woei Ho. Online robot guidance and navigation in non-stationary environment with hybrid hierarchical reinforcement learning. *Engineering Applications of Artificial Intelligence*, 114:105152, 2022. 3
- [71] Hao Zhu, Raghav Kapoor, So Yeon Min, Winson Han, Jiatai Li, Kaiwen Geng, Graham Neubig, Yonatan Bisk, Anirudha Kembhavi, and Luca Weihs. Excalibur: Encouraging and evaluating embodied exploration. In *Proceedings of the IEEE/CVF Conference on Computer Vision and Pattern Recognition*, pages 14931–14942, 2023. 6

# Right Place, Right Time!

## Generalizing ObjectNav to Dynamic Environments with Portable Targets

### Supplementary Material

#### Supplementary Material

#### 8. P-ObjectNav Definition

In this section, we repeat the definition of P-ObjectNav for convenience.

The objective of ObjectNav as defined in literature [4] is to navigate to a target object specified by a target label in a previously unseen environment. Prior techniques [17, 19, 61] for solving this can be broadly broken down into two components 1) Sequential Decision Making and 2) Visual Grounding. The latter decides how the agent should navigate at each waypoint, while the former decides where the target object lies in the final image. Our work introduces **two key changes** to this setup -

1. We add spatial and temporal dynamism to the embodied environment.
2. There is no singular intended target per epoch ("Get to the chair", for example), but rather the task is to find as many portable targets as possible within the epoch.

We define P-ObjectNav as "*Navigating to the most portable objects possible from a given starting point within a fixed number of timesteps.*"

#### 9. Dataset Details

While the P-ObjectNav agents introduced in Section 2 tackle the *temporal* dynamism, i.e., identifying *where* and *when* the target object is likely to lie at a particular location, visual grounding is a separate task tackling *spatial* dynamism. An ideal agent performs both these tasks *simultaneously*, verifying at each timestep if a portable target exists by running a grounding model. As navigation decisions are not directly impacted by the performance of a grounding model, we study temporal and spatial dynamism independently.

The P-ObjectNav dataset contains temporal and spatial modifications on the Matterport3D scans. Further, we provide code and useful tools for implementing these modifications.

For the spatial placement, we provide a dataset of 10,500 modified images taken across 10 randomly chosen Matterport3D scans, with 21 portable objects randomly oriented and positioned 5 times within each image. Table 4 summarizes the different Matterport3D scans chosen. To emulate realism such that the portable objects are not floating in the sky or on the ceiling, they are placed on a large segmented area below the center of the image. We also provide

Scan ID	# of Nodes	# of Edges	# of Rooms
QUCTc6BB5sX	145	248	28
8194nk5LbLH	20	32	6
TbHJrupSAjP	114	221	28
2azQ1b91cZZ	215	531	30
oLBMNvg9in8	111	185	31
zsNo4HB9uLZ	53	84	17
EU6Fwq7SyZv	78	166	19
X7HyMhZNoso	84	143	25
x8F5xyUWy9e	43	86	10
Z6MFQCViBuw	58	91	18

**Table 4.** Summary statistics of scans used for Table 3, including each scan’s ID, number of nodes, edges, and rooms. If a scan has multiple rooms of the same type (e.g. two bathrooms), each instance is counted separately from the total. Figure 3 utilizes only scan QUCTc6BB5sX.

the bounding boxes pertaining to the portable object in each image.

#### 9.1. Temporal: Implementing Object Placement Strategies

In this section, we give more details on how we implemented the dynamic Matterport3D environment.

##### Matterport3D Modifications:

Each Matterport3D (MP3D) scan represents a household environment consisting of a set of panoramic view points. Along with the viewpoints (or nodes), we are also given the exact 3D position as well as the relative distance between them. For modifying the MP3D environment, we first construct topological graphs of each scan, with nodes containing the position and the panoramic image, and edges containing relative distance between them. We consider 10 different scans chosen from the REVERIE [41] and R2R [3] unseen validation splits for inference. We choose scans according to these datasets as they contain a variety of rooms for us to populate (Refer Table 1 in the main paper).

The nodes of the topological graphs are then updated at each timestep with the portable objects according to the object placement scenario that has been chosen.

##### Strategy Overview:

We compute trajectories of the portable objects in an offline manner. For a fixed random seed  $s$  and for each portable object  $o_p \in O_p$ , we create a sequence of nodes from the graph. In the random transit scenario, we choose any node

in the graph. In the routine and semi-routine scenarios, we only choose nodes from plausible rooms. If the node chosen is not the same as the current node, we find the shortest path between the current node and the target node and add the nodes in the path to the sequence representing the trajectory. Once  $o_p$  gets to the target node, it stays there for either 2 or 3 timesteps, determined by a random number generator. For each timestep  $o_p$  stays at the node, we add the node to the trajectory sequence. After the staying period is over we select a new node and repeat the process until we hit  $T$  timesteps.

We take the resulting trajectories and restructure the data to model an evolving graph over a period of  $T$  timesteps. The resulting structure is a nested dictionary representing the changing graph. The keys of the outer dictionary are the timesteps  $[1, \dots, T]$ . The inner dictionary for each timestep  $t$  has the node string ids as the keys and the values are the list of portable objects at that node at  $T$ . At each timestep  $t \in [1, \dots, T]$  when the agent reaches a node, we simply use  $t$  and the node id to retrieve the list of portable objects the agent is currently observing.

## 9.2. Spatial: Implementing Visual Grounding

In this section, we talk about our strategy for spatial placement of multiple portable target objects on MP3D scenes. After placing portable objects at various locations, we perform visual grounding using three Open-World Object Detection models for inference. We also show further ablations using VLMs.

### Generating Spatial Data:

We randomly choose 100 skybox images taken across the 10 MP3D scans mentioned in the previous subsection. While selecting these images are not of the ceiling or the floor, and have objects pertaining everyday scenes. We then pick stock images of all the 21 portable objects present in Table 1 of the main manuscript. These images are shown in Figure 9.

For each of the skybox images, we first run FastSAM [65] and segment out the largest regions below the center of the image. We then randomly orient the portable object and place it at a random position on one of these segments. Choosing segments below the center of the image is necessary to ensure that the portable objects being placed follow commonsense, and do not hang in the ceiling. This is done 5 times for each of the 21 objects on 100 images, to get 10500 images in total. While placing the images, we also store the boundaries of the overlay as the ground truth bounding box for computing Intersection over Union (IOU) scores.

Examples of this generated data is shown in Figure 7. Note that the same image can have multiple target segmentations (*bed* and *cushion* for example), with different objects placed on them at different orientations.

## Open-World Visual Object Grounding

We perform Visual Grounding on the spatial placement dataset using various Open-Vocabulary Object Detection Models. For each model, we assess the **Detection Coverage**, which is the percentage of images where the portable object was found, the **Detection Accuracy**, the accuracy of the predicted detections, and finally **Mean IOU**, which gives us the overlap between the ground truth bounding box of the placed target and the predicted box. The results for this are shown in Table 5.

We make some interesting observations. OWL-ViT [35] outperforms GLIP [27] and YOLO-World [10] when it comes to Detection Coverage, which means that it consistently detects an object, irrespective of whether it is right or wrong on the image. This is evident since it takes a target object label is given as a prompt to OWL-ViT, so it detects something in the image, even if the confidence is low. Figure 4 shows some examples of this.

GLIP, while having lower detection coverage, has a perfect detection accuracy, meaning that when GLIP does detect something, it usually is correct. The high MIOU score associated with GLIP also corroborates with this fact. Figure 5 shows some example results of this.

We infer the YOLO-World model with custom vocabulary consisting of all the portable object names. Despite this, YOLO still performs the worst among the three, with poor detection accuracy and coverage. Figure 6 showcases one of these results. Notice that in the first image screw-driver is grounded at the right location, but the label is “Cow”. In the second image, both the predicted target (fire hydrant) and the grounding is wrong.

We note that the poor detection as measured by MIOU could be a result of unnatural scenes that are different from those which these models might have been trained on. Beyond this, grounding small, portable targets that could be present on various surfaces in a household environment still remains a challenge. We will be releasing this dataset to foster research in this area.

## 9.3. Spatial Reasoning with Vision Language Models (VLMs)

We perform visual grounding using 4 popular Vision Language Models (VLMs): InstructBLIP [32], LLaVA 1.5 [31] and GPT-4o [1]. For InstructBLIP, we experiment with two different language backends: Flan-T5, which has been fine-tuned on various language tasks including question answering, and Vicuna-13B, which has been trained specifically on conversational data.

Figure 10 illustrates the images we pass to these models to validate their spatial reasoning capability. Given an image containing a small portable target for grounding, we first paste a number grid from  $[1 - 9]$  onto the image. Prior research by Sathyamoorthy et. al [49] and Nasiriany et. al



(a) Portable Target: Bowl



(b) Portable Target: Playing Cards

**Figure 4. OWL-ViT Detection Failures:** Note the poor detection accuracy of OWL-ViT. On both images, it completely misses the object when prompted with a text containing the target label. We attribute these failures to unnatural images being generated by pasting target objects onto the scene.



(a) Portable Target: Playing Cards



(b) Portable Target: Dumbbells

**Figure 5. GLIP Detection Accuracy:** Note the superior detection accuracy, despite the low coverage on GLIP. On the image on the left and right, playing cards and dumbbells are detected correctly with a high accuracy.

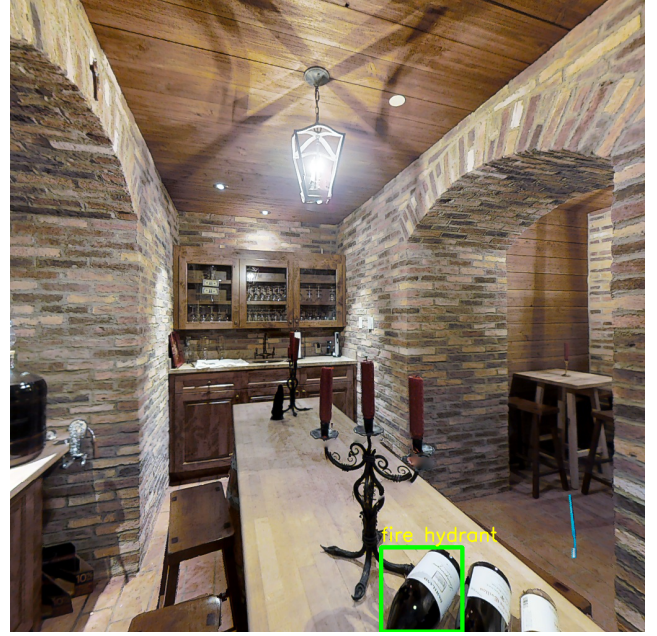
[38] has utilized this technique to guide robots in indoor as well as outdoor scenarios.

In our case, we evaluate a subset of 1000 images in our dataset containing various objects by asking each image the

query - “Where is the *<objects>* in this image? Reply with the corresponding grid number from [1-9].”, and then evaluate the response we get with the ground truth. Since we create the dataset by pasting target objects onto them, this is



(a) Portable Target: Screwdriver



(b) Portable Target: Toothbrush

**Figure 6.** YOLO Detection Failures: Note the poor detection accuracy of YOLO. On the image on the left, the screwdriver is grounded correctly, but the object name predicted is “Cow”. On the image on the right, YOLO completely misses the target object toothbrush, and instead grounds and labels something else.

Approach	Detection Coverage	Detection Accuracy	MIOU
<b>OWL-ViT</b> [35]	<b>100%</b>	3.04%	0.352
<b>GLIP</b> [27]	7.11%	<b>100%</b>	<b>0.489</b>
<b>YOLO-World</b> [10]	32.94%	0.2%	0.130

**Table 5.** Comparison of Open-World Object Detection Approaches

readily available to us. Table 6 presents the accuracies for this task the various VLMs.

Model	Accuracy (%)
InstructBLIP + Vicuna-7B	15.38
InstructBLIP + Flan-T5-XL	4.32
LLaVA v1.5 + Vicuna 13B	58.62
GPT 4o-mini	75.89
GPT 4o	<b>98.32</b>

**Table 6. VQA Model Accuracies:** Note the superior performance of GPT 4o on our number grid based spatial reasoning task. The remaining VLMs show inferior performance, with a Vicuna backend performing better than the Flan one; this can be attributed to Vicuna being predominantly trained on conversational data that might contain such queries.

## 10. Experimental Details

### 10.1. LGX Inference

We utilize the official implementation of LGX<sup>1</sup> and incorporate it into our modified MP3D environment. Briefly, at each timestep, LGX scans the node for objects, and asks an LLM for directions to reach a target. In our case, we seek to maximize finding portable targets. As such, we prompt GPT-4 with the following base prompts -

**System Prompt** - “I am a smart robot trying to find as many portable objects as I can at home.”

**User Prompt** - “Which object from `<OBJECT_LIST>` should I go towards to find a new portable object? Reply in ONE word.”

The `<OBJECT_LIST>` here contains a set of objects that have been detected using YOLO-v8, as proposed in LGX. Additionally, we if a portable object is present at a certain node at a given timestep, we add it to this list.

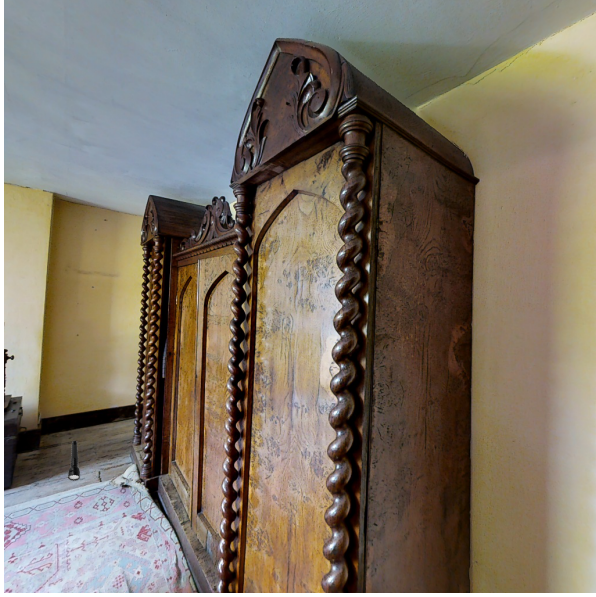
<sup>1</sup><https://github.com/vdorbal/LGX>



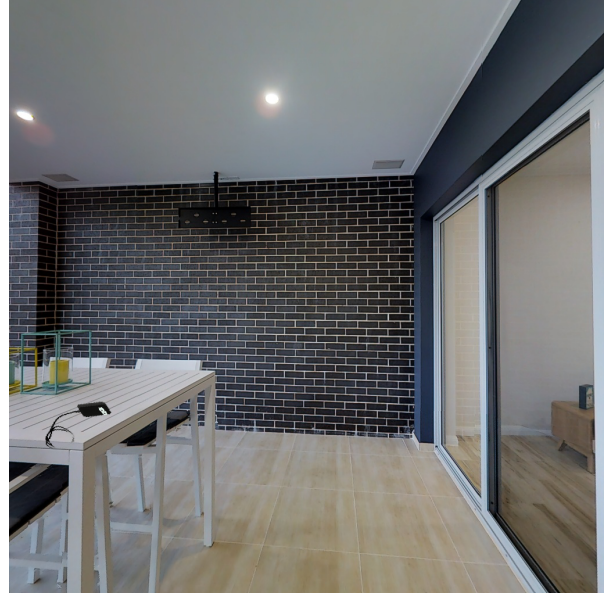
(a) Dice on Bed



(b) Mug on Cushion



(c) Flashlight on Floor



(d) Charger on Table

**Figure 7.** Various Spatial Placement in our Dataset: Figures (a) and (b) look at different arrangements of objects in the same room. Figure (c) shows a flashlight on the floor, and figure (d) shows a charger on the table. We cover various orientations and rotations of portable objects being placed on various objects in different MP3D scans.

The LLM then predicts a target object from the list, which is mapped to an adjacent node using our customized MP3D functions.

For the **memory-enhanced LGX** case, we modify the System Prompt, with memory. We ask -

**System Prompt:**

“I have seen the following objects and taken the following actions so far -

1. <OBJECT\_LIST>: ACTION

2. <OBJECT\_LIST>: ACTION  
...

**User Prompt:**

“Which object from <OBJECT\_LIST> should I go towards to find a new portable object? Reply in ONE word.”

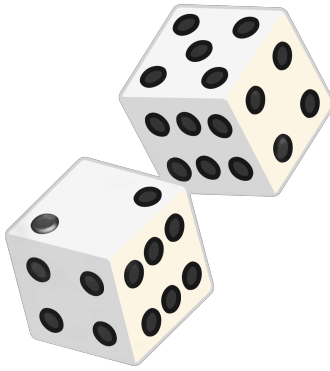
## 10.2. PPO Training

In this section, we repeat the details of the PPO training:

- Current timestep,  $t \in T$



(a) bowl



(b) dice



(c) dumbbell



(d) flashlight



(e) glasses



(f) hat



(g) salt and pepper shakers



(h) screwdriver



(i) toothbrush



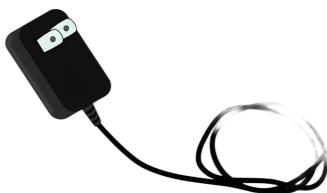
(j) remote



(k) playing cards



(l) phone



(m) phone charger



(n) notebook



(o) mug



**Figure 9. Portable Objects:** A list of all the 21 portable objects we consider for our task.



**Figure 10.** We evaluate the spatial reasoning capabilities of VLMs in grounding small portable targets in houses. The question we ask is “What is the closest number to the <INSERT OBJECT> in this image?” and it answers with a number.

- Index of the current node,  $n_t$  from a list of all nodes in the environment graph
- A list with each index corresponding to a node, and the element at a given index being the number of objects at

the corresponding node at  $t$

- Another list with each index corresponding to a node. The element at a given index is 1 if the corresponding node is an immediate neighbor to the current node and 0 otherwise.

The PPO agent then outputs the index of the node it wants to travel to for the next timestep  $t + 1$ . Let  $O_{t-1}$  be the set of distinct portable objects the agent has seen up to time  $t - 1$ . The reward is the number of new objects it has found at the current node  $n_t$  that are not in  $O_{t-1}$ . Formally the reward at timestep  $t$  is  $|O(n_t) \setminus O_{t-1}|$ . We also note that this structure requires access to a map of the environment and oracle knowledge of the number of new objects at each node at each timestep. We use StableBaseline3 with neural network parameterizations of both policy and critic.

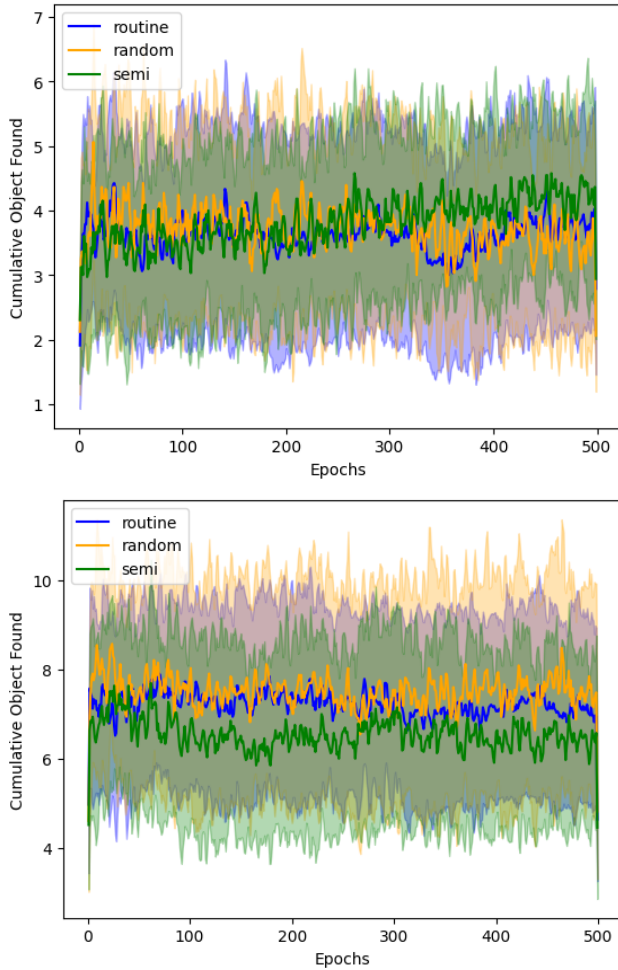


**Figure 11.** PPO training for 500 epochs in routine, semi-routine, and random transit scenarios. Object density of the initial local graph is (TOP) 1 and (BOTTOM) 4.

**Increasing epochs for PPO Training:** To better analyze the effect of transit scenarios on learning, we ran PPO train-

ing for 500 epochs. Figure 11 shows the results of PPO training for each transit scenario with object density (TOP) 1 and (BOTTOM) 4 of the initial local graph. We do not see a noticeable difference in COF between transit scenarios as in Table 3. One potential explanation is the possibility that our routine case was too difficult for a PPO agent to learn and it converged to a policy that was randomly guessing locations to hop to.

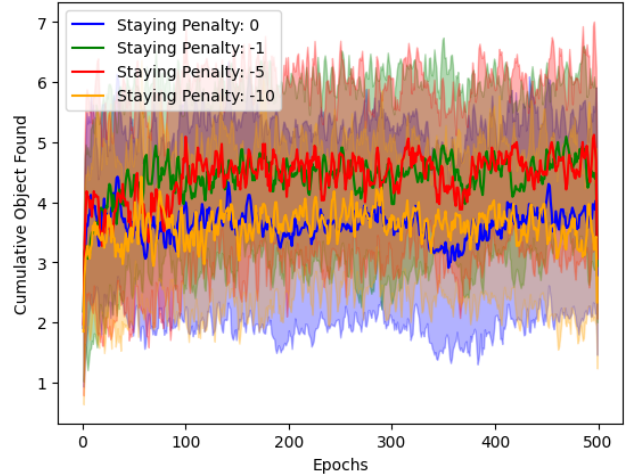


**Figure 12. Routine Case with Penalty:** We add various negative rewards (-1, -5, -10) for going to a node that it has been within the past five timesteps to encourage exploration. We report the mean of the 10 runs with different starting room with the shaded regions representing a 95% confidence interval. Negative rewards seem to potentially improve performance.

**Effect of Negative Rewards:** We experiment with negative rewards for PPO. Figure 12 shows results from our experiments with negative rewards for going to a node that had been visited in the last 5 timesteps. We see a slight increase in performance when applying a -1 or -5 penalty to the reward structure, suggesting that the agent could be encouraged to explore and find new objects with a more complex reward structure.

## 11. Code and Dataset

We provide an anonymous link to our Code: <https://anonymous.4open.science/r/PObjectNav-1C6D>. The dataset will be present as a downloadable link in the code repository.

Furthermore, please see the attached video in the zip file for more information and demonstrations.